A Precise Positioning Method with Integration of GNSS and Doppler Shift Based Positioning using LEO Satellite

M. Humayun Kabir
Electrical and Computer Engineering
Ajou University
Suwon, Republic of Korea
humayun@ ajou.ac.kr

Md. Ali Hasan
Dept. of AI Convergence Network
Ajou University
Suwon, Republic of Korea
mdalihasan@ajou.ac.kr

Wonjae Shin
Electrical and Computer Engineering
Ajou University
Suwon, Republic of Korea
wjshin@ajou.ac.kr

***Abstract*— Global Navigation Satellite System (GNSS) utilizes medium earth orbit (MEO) and geostationary earth orbit (GEO) satellites with time difference of arrival (TDOA) based multilateration technique to determine position. Due to the long orbital altitude of GNSS satellites from the earth surface, the signal strength is very low. This low signal is also remarkably attenuated and reflected by nature (tall trees) and buildings that induces large errors in pseudorange measurements. In contrast, the closer earth orbit of LEO provides strong signal power and high Doppler frequency shift range (±40kHz). This is advantageous to develop Doppler shift-based positioning algorithm. However, using the iterative method of Doppler shift positioning the initial receiver position plays a vital role in ensuring convergence. To face this challenge, we have utilized the positioning outcome of GNSS as an initial receiver position and then utilized the Doppler shift-based algorithm to estimate the more precise position. Experimental results show that the proposed approach reduces positioning error significantly compared to the individual GNSS method.**

Keywords—Doppler-Shift, GNSS, TDOA, Multilateration.

I. INTRODUCTION

Global navigation satellite system (GNSS) may block in some geographical area such as large urban canyon, desert, forest due to its low signal power. The signals are attenuated and reflected by obstacles while propagating to the receiver. Moreover, present GNSS constellations are inefficient to provide good relative geometry line-of-sight (LOS) vector. On the other hand, a thousand of space vehicles (SVs) into LEO mega-constellations (i.e. Oneweb, Kuiper, Starlink, etc.) made a renaissance in LEO-based positioning, navigation, timing, remote sensing and communication (LEO-PNTRC) [1]. It has relative closer proximity of Earth compared to geostationary earth orbit (GEO) and medium earth orbit (MEO) satellites in GNSS. For example, LEO satellites are on a circular orbit at 780 Km altitude which makes their signal much more than 20dB stronger than that of GNSS signals. LEO constellations come up with sufficient geometric diversity for the LOS vectors [2]. User terminal (UT) can see multiple LEO satellites over the horizon and select the best one for communication and registration process in the network. LEO signals are more capable to penetrate indoors and to offer good coverage in deep urban canyons. The latency time has been reduced from 700ms to 100ms. Moreover, the closer earth orbit of LEO provides strong signal power and high Doppler frequency shift ranges from ±40kHz [3]. As a result, LEO satellite constellation utilizing Doppler shift-based positioning can be an alternate to present pseudorange based GNSS.

However, to ensure convergence in the LEO based Doppler shift positioning, the initial receiver position error plays a important rule. If we fail to set the initial point, then the positioning solution may not converge. For example, the initial positioning error should be less than 300 km when the satellites orbit is at an altitude of 550 km [4]. In order to address this challenge, we have utilized the GNSS positioning outcome as the initial guess for the LEO-based Doppler positioning to get precise user position.

II. SYSTEM MODEL

GNSS uses pseudorange based positioning over decades. The poor geometry between satellite and receiver effects the positioning accuracy in conventional GNSS. The inclusion of LEO satellite constellations enhance the capacity and performance of conventional geosynchronous orbit (GEO) and medium earth orbit (MEO) based GNSS. There is a high probability of poor geometric dilution of precision (GDOP) in GNSS scenarios. Hence, Doppler positioning can be integrated with pseudorange based GNSS positioning where the role of the GNSS is to share the positioning outcome that can be used by the Doppler shift-based positioning as an initial positioning guess. This approach can overcome the limitation where the positioning solution is not converged in Doppler shift-based positioning method. Fig. 1 shows the system model for the proposed method. Assume that UT has the ability to receive navigation messages from GNSS as well as estimate the Doppler shift from LEO satellites. Moreover, it can access the Two-line Element (TLE) [5] which contains the satellite velocity, position, and orbital information.

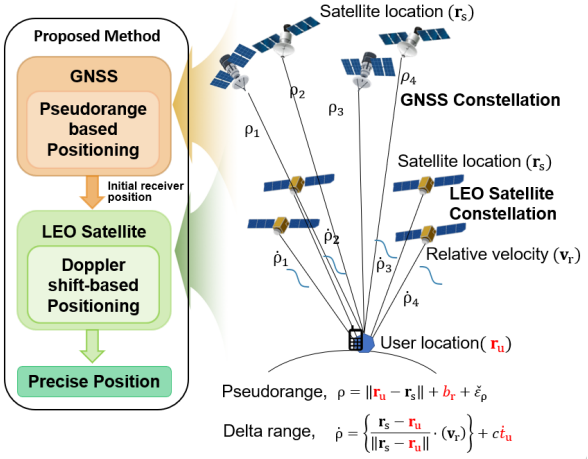

Fig. 1. System model of the proposed precise positioning method.

III. PROPOSED METHODS

Pseudorange based positioning:

Most GNSS systems adopt the time-of-arrival (TOA) based ranging techniques to determine the user position [3]. The pseudorange measurements for the m^{th} satellite is

$$\rho^{[m]} = \left\|\mathbf{x} - \mathbf{x}^{[m]}\right\| + c\partial t_{\text{r}} - c\partial t_{\text{s}} + cI^{[m]} + cT^{[m]} + \varepsilon_{\rho}^{[m]}, \quad (1)$$

where $\mathbf{x} = [x, y, z]^T$ is the receiver position and $\mathbf{x}^{[m]} = \left[x^{[m]}, y^{[m]}, z^{[m]}\right]^T$ is the position of the m^{th} satellite in earth center earth fixed (ECEF) frame, ∂t_{r} is the receiver's clock offset (sec), and ∂t_{s} is the satellite's clock offset (sec). $I^{[m]}$ is the ionospheric delay (sec); $T^{[m]}$ is the tropospheric delay (sec); ε_{ρ}^{m} is the error in the range due to various sources, including receiver noise, multipath, orbit prediction (meters).

After compensating the ionospheric, tropospheric error, (1) can be written as follows

$$\rho_c^{[m]} = \left\|\mathbf{x} - \mathbf{x}^{[m]}\right\| + b_r + \breve{\varepsilon}_{\rho}^{[m]}, \quad (2)$$

where $b_r = c\partial t_r$ is the error in range (in meters) due to the receiver's clock bias and $\breve{\varepsilon}_{\rho}^{m}$ is the total effect of residual errors.

Eq. (2) can be linearized using Taylor series to the current best estimation, $\mathbf{x}_{\text{EST}} = [x_{\text{EST}}, y_{\text{EST}}, z_{\text{EST}}]^T$ and apply iterative method to get the position of user $\mathbf{x} = [\text{x}, y, z]^T$.

$$\delta\rho_{\text{c}}^{m} = (\mathbf{G}_{\text{EST}}^{\text{m}})^T\delta\mathbf{x} + \delta b_{\text{r}} + \tilde{\varepsilon}_{\rho}^{\text{m}}, \quad (3)$$

where $\delta\rho_{\text{c}}^{m} = \rho_{\text{c}}^{m} - \rho_{c,\text{EST}}^{m}$, $\delta b_r = b_r - b_{r,\text{EST}}$, $\delta\mathbf{x} = \mathbf{x} - \mathbf{x}_{\text{EST}} = [x, y, z]^T - [x_{\text{EST}}, y_{\text{EST}}, z_{\text{EST}}]^T$, LOS unit vector $\mathbf{G}_{\text{EST}}^{[m]} = \left[g_x^{[m]} \quad g_y^{[m]} \quad g_z^{[m]}\right]$ [6].

For M satellites, the linearized pseudorange measurements are

$$\delta\boldsymbol{\rho}_{\mathbf{c}} = \begin{bmatrix} \delta\rho_c^1 \\ \delta\rho_c^2 \\ \vdots \\ \delta\rho_c^M \end{bmatrix}_{M\times 1} = \begin{bmatrix} \mathbf{G}_{\text{EST}}^1 & 1 \\ \mathbf{G}_{\text{EST}}^2 & 1 \\ \vdots & \vdots \\ \mathbf{G}_{\text{EST}}^M & 1 \end{bmatrix}_{M\times 4} \begin{bmatrix} \delta\mathbf{x} \\ \delta b_{\text{r}} \end{bmatrix}_{4\times 1} + \begin{bmatrix} \tilde{\varepsilon}_{\rho}^1 \\ \tilde{\varepsilon}_{\rho}^2 \\ \vdots \\ \tilde{\varepsilon}_{\rho}^M \end{bmatrix}_{M\times 1} \quad (4)$$

The positioning accuracy depends on a number of factors (elevation angles, NLOS, measurement noise). Using weighting factors, we can get the weighted least squares (WLS) solution

$$\begin{bmatrix} \delta\hat{\mathbf{x}} \\ \delta\hat{b}_{\text{r}} \end{bmatrix} = (\mathbf{G}^{\text{T}}\mathbf{W}\mathbf{G})^{-1}\mathbf{G}^{\text{T}}\mathbf{W}\delta\boldsymbol{\rho}_{\mathbf{c}}, \quad (5)$$

where $\mathbf{W}$ is the weighting matrix.

The improved estimates of their states are

$$\hat{\mathbf{x}} = \mathbf{x}_{\text{EST}} + \delta\hat{\mathbf{x}},$$
$$\hat{b}_{\text{r}} = b_{\text{r,EST}} + \delta\hat{b}_{\text{r}} \quad (6)$$

The estimated $\hat{\mathbf{x}}$ is shared to the Doppler shift-based positioning as an initial position in (13).

Doppler shift-based positioning:

Doppler shift is the change of frequency of the electromagnetic signal due to the relative motion between the satellite and the UT [2]. Assume satellite (S) and receiver (R) are moving close to each other. At time t_0 and t satellite location is S_{t_0} and S_t. P and Q are the sub-satellite points of S_{t_0} and S_t. The Doppler shift can be expressed as

$$f_{\text{d}} = \frac{\dot{r}}{\lambda} \quad (7)$$

where f_{d} = Doppler shift, $\dot{r}$ = rate of change of LOS vector between satellite and user terminal, $r = \|\mathbf{r}_{\text{s}} - \mathbf{r}_{\text{u}}\|$, $\mathbf{r}_{\text{s}}$ = position of satellite, $\mathbf{r}_{\text{u}}$ = position of receiver, $\lambda = \frac{c}{f}$ wavelength of the transmitter frequency of satellite, f = frequency of the transmitter and c = velocity of light.

Differentiating r with respect to time t, $\dot{r}$ can be revealed as

$$\dot{r} = \left\{\frac{\mathbf{r}_{\text{s}} - \mathbf{r}_{\text{u}}}{\|\mathbf{r}_{\text{s}} - \mathbf{r}_{\text{u}}\|} \cdot (\mathbf{v}_{\text{s}} - \mathbf{v}_{\text{u}})\right\} \quad (8)$$

The error induced in the estimation of received frequency can be written as

$$\delta f = \dot{t}_{\text{u}} f, \quad (9)$$

where $\dot{t}_{\text{u}}$= receiver clock drift.

Assume the user terminal received the frequency f_{u} from the satellite. Then the doppler shift is

$$f_{\text{u}} - f = f_{\text{d}} + \delta f + \varepsilon_{\text{f}}, \quad (10)$$

where ε_{f} = measurement noise.

Substituting the values of f_{d} and δf in Eq. (10) and multiply by $\frac{c}{f}$ gives delta range $\dot{\rho}$ and can be expressed as

$$\dot{\rho} = \left\{\frac{\mathbf{r}_{\text{s}} - \mathbf{r}_{\text{u}}}{\|\mathbf{r}_{\text{s}} - \mathbf{r}_{\text{u}}\|} \cdot (\mathbf{v}_{\text{s}} - \mathbf{v}_{\text{u}})\right\} + c\dot{t}_{\text{u}} + \tilde{\varepsilon}_{\text{f}} \quad (11)$$

The receiver position and drift vector $\mathbf{x} = [\mathbf{r}_u^{\boldsymbol{T}}, c\dot{t}_u]^T = [x_u, y_u, z_u, c\dot{t}_u]^T$, the delta range measurement vector $\dot{\boldsymbol{\rho}} = \left[\dot{\rho}^{[1]}\ \dot{\rho}^{[2]} \cdots \dot{\rho}^{[n]}\right]^T$, and the delta range residuals function $\delta\dot{\boldsymbol{\rho}}$ yields

$$\delta\dot{\boldsymbol{\rho}} = \begin{bmatrix} \frac{\mathbf{r}_s^{[1]} - \mathbf{r}_u}{\left\|\mathbf{r}_s^{[1]} - \mathbf{r}_u\right\|} \cdot \left(\mathbf{v}_s^{[1]} - \mathbf{v}_u\right) + c\dot{t}_u - \dot{\rho}^{[1]} \\ \frac{\mathbf{r}_s^{[2]} - \mathbf{r}_u}{\left\|\mathbf{r}_s^{[2]} - \mathbf{r}_u\right\|} \cdot \left(\mathbf{v}_s^{[2]} - \mathbf{v}_u\right) + c\dot{t}_u - \dot{\rho}^{[2]} \\ \vdots \\ \frac{\mathbf{r}_s^{[n]} - \mathbf{r}_u}{\left\|\mathbf{r}_s^{[n]} - \mathbf{r}_u\right\|} \cdot \left(\mathbf{v}_s^{[n]} - \mathbf{v}_u\right) + c\dot{t}_u - \dot{\rho}^{[n]} \end{bmatrix}, \quad (12)$$

where n is the number of satellites.

$\delta\dot{\boldsymbol{\rho}}$ is a function of $g(\mathbf{x}) \in \mathbb{R}^n$, n = number of measured delta ranges. $\delta\dot{\boldsymbol{\rho}}$ measures the difference between the predict delta range with the measured delta range using argument $\mathbf{x}$. The first order Taylor series is used to linearize the delta range residual function $g(\mathbf{x})$. $\hat{\mathbf{x}}_k$ is taken from (6).

$$g(\hat{\mathbf{x}}_k + \delta\mathbf{x}) \approx g(\hat{\mathbf{x}}_k) + \frac{\partial g(\mathbf{x})}{\partial(x)}\Big|_{x=\hat{x}_k}\delta x + \frac{\partial g(\mathbf{x})}{\partial(y)}\Big|_{y=\hat{y}_k}\delta y + \frac{\partial g(\hat{\mathbf{x}})}{\partial(z)}\Big|_{z=\hat{z}_k}\delta z + \frac{\partial g(\hat{\mathbf{x}})}{\partial(t_u)}\Big|_{t_u=\hat{t}_{u_k}}\delta t \quad (13)$$

To get the derivative of function $g(\mathbf{x})$, the right-hand side of the Eq. (13) is set to zero such that

$$g(\hat{\mathbf{x}}_k) + \frac{\partial g(\hat{\mathbf{x}}_k)}{\partial(\mathbf{x})}\delta\mathbf{x} = 0 \quad (14)$$

Weighting factors are considered based on the C/N_0 can apply with the measurement of residual accordingly. Thus, using iterative WLS, the $\delta\boldsymbol{x}$ can be calculated as

$$\delta\mathbf{x} = -\left(\frac{\boldsymbol{\partial} g(\hat{\mathbf{x}}_k)}{\boldsymbol{\partial}(\mathbf{x})}^T \mathbf{W} \frac{\boldsymbol{\partial} g(\hat{\mathbf{x}}_k)}{\boldsymbol{\partial}(\mathbf{x})}\right)^{-1} \frac{\boldsymbol{\partial} g(\hat{\mathbf{x}}_k)}{\boldsymbol{\partial}(\mathbf{x})}^T \mathbf{W}\, g(\hat{\mathbf{x}}_k),$$
$$\hat{\mathbf{x}}_{k+1} = \hat{\mathbf{x}}_k + \delta\mathbf{x}, \quad (15)$$

where $\mathbf{W}$ is a diagonal matrix with diagonal elements $\{w_1, w_2, \ldots, w_k\}$. The estimation for the position and drift is updated iteratively until the $\delta\mathbf{x}$ reaches below the expected range.

In Doppler positioning user terminal needs to know the velocities and positions of satellites. NORAD updates the TLE which contains orbital mechanics [5]. We used the TLE file to determine the position and velocity of LEO satellite. Fig. 2 shows the TLE file and LEO constellation simulated using TLE file considering user terminal at Ajou University,

Republic of Korea (37°16'56.9382"N, 127°02'36.2184"E) at a certain time.

```
STARLINK-1062
1 44767U 19074BG  23229.04306954  .00006374  00000+0  44632-3 0  9999
2 44767  53.0540 106.8923 0000936  95.1131 264.9965 15.06405739207341
STARLINK-1146
1 45094U 20006BC  23228.71317669  .00003938  00000+0  28311-3 0  9997
2 45094  53.0543 128.3727 0001607  96.0543 264.0629 15.06399916196302
STARLINK-1135
1 45049U 20006F   23228.12974757  .00007780  00000+0  33030-3 0  9992
2 45049  53.0900 138.8964 0006825 110.1469 250.0262 15.24007545196100
STARLINK-1126
1 44951U 20001AP  23228.12078832  .00027465  00000+0  52143-3 0  9995
2 44951  53.0197 133.2995 0003895 244.7236 115.3368 15.48105034201297
STARLINK-1172
1 45074U 20006AG  23229.04769636  .00014762  00000+0  10075-2 0  9991
2 45074  53.0551 146.8803 0001322  94.2312 265.8828 15.06411734196052
```

(a)

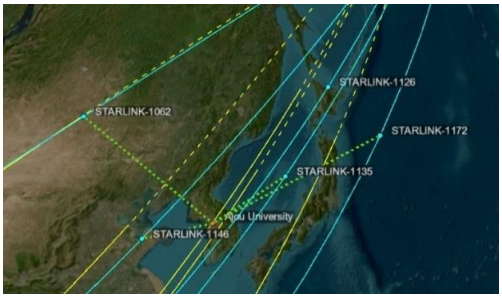

(b)

Figure 2. a. TLE file, b. A part of the Starlink LEO satellites orbits used in Doppler shift-based positioning.

IV. Experimental Results and Discussion

The GNSS measurements can be accessible through Android (version 7 and others upgrade versions) OS. There has been remarkable improvement in the GNSS research community. This expands the scope of developing a new algorithm for improving the positioning performance. The raw GNSS data of 150-250s durations were captured using Samsung SM-A515F smartphone having Android (version 10) operating system [7]. Then WLS based position estimation is done using GNSS measurement using MATLAB based GPS-measurement tools [8]. We have considered this position as initial guess for Doppler shift-based position estimation.

The true location is 37°16'56.9382"N, 127°02'36.2184"E, near the statue of Pioneer, at Ajou University, Suwon, Seoul in South Korea. Fig. 3 shows the comparison of positioning error between pseudorange based positioning with the proposed method (integration of GNSS with Doppler shift-based LEO Sat.) in 3-D. The maximum, minimum, and mean 3-D positioning error of pseudorange-based positioning using GNSS satellite are 43.19m, 1.28m, and 15.07m respectively. The maximum, minimum, and mean 3-D positioning error of proposed method are 20.85m, 1.09m, and 6.53m respectively. The comparison of positioning error between pseudorange based positioning with the proposed method in north east down (NED) coordinate is shown in fig. 4. The mean ± standard deviation positioning error of conventional pseudorange based method in north, east, down direction is 5.27±6.78m, 3.47±4.41m, and 13.68±15.54m respectively. The mean ± standard deviation positioning error of proposed method in north, east, down direction is 4.49±5.59m, 3.94±4.98m, and 2.64±3.42m respectively.

V. Conclusion

This paper presents a new approach for precise positioning using integration of Doppler shift-based positioning technique utilizing LEO constellation with the existing pseudorange based positioning approach by GNSS. From the experimental results it is assumed that the proposed method outperforms pseudorange based conventional positioning method utilized by the existing GNSS.

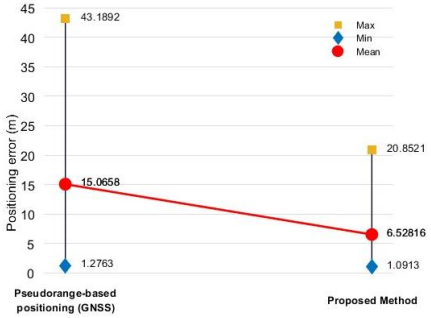

Figure 3. Comparison of positioning error between pseudorange-based positioning with the proposed method in 3-D.

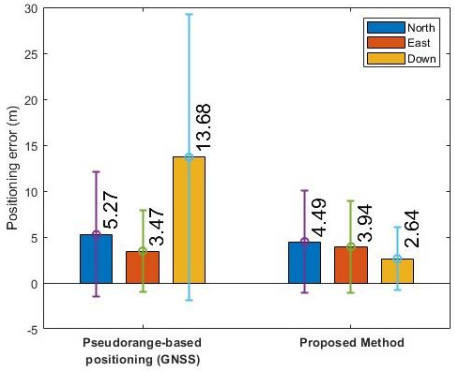

Figure 4. Comparison of positioning error between Pseudorange-based positioning with the proposed method in NED coordinate.

Acknowledgment

This work was supported in part by the National Research Foundation of Korea (NRF) grants (No.2021R1A4A1030775, No.2022R1A2C4002065) and in part by the Institute of Information & communications Technology Planning & Evaluation (IITP) grants (No. 2023-2018-0-01424).

References

[1] L. Bofeng, G. Haibo, G. Maorong, N. Liangwei, Y. Shen, and H. Schuh. "LEO enhanced Global Navigation Satellite System (LeGNSS) for real-time precise positioning services." Advances in space research 63, no. 1 (2019): 73-93.

[2] A. Noureldin, T. B. Karamat, and J. Georgy, "Fundamental of Inertial Navigation Satellite-based Positioning and their Integration," *Springer*, 2013, pp.67, pp. 97-110.

[3] M. H. Kabir and W. Shin, "LEO Satellite Based Positioning: An Evaluation on Doppler Frequency and Doppler Frequency Rate from Receiver-Side," in Proc. 32nd Joint Conference on Communications and Information (JCCI 2022), 2022.

[4] C. Shi, Y. Zhang, and Z. Li, "Revisiting Doppler positioning performance with LEO satellites," GPS Solutions, vol. 27(3), 126, 2023.

[5] D. A. Vallado and P. Cefola, "Two-line element sets - Practice and use," in Proc. 63rd International Astronautical Congress, Naples, Italy, 2012, pp. 1-14.

[6] M. H. Kabir, M. A. Hasan, and W. Shin, "Performance Analysis of Positioning Algorithm Using Raw GNSS Measurements of Smartphone," KICS summer conference, 638-639, 2022.

[7] M. H. Kabir, S. Lee, and W. Shin, "Performance evaluation of GNSS positioning with Geometric Dilution of Precision," In 13th International Conference on Information and Communication Technology Convergence (ICTC) (pp. 910-912). IEEE, (2022, October).

[8] S. Kuznetsov, M. Fu, D. Herenu, M. Khaider, and F. V. Digglen, Google/gps-measurement-tools, https://github.com/google/gps-measurement-tools (last access on 29 August 2023).